BIOCHEMISTRY
including biophysical chemistry & molecular biology
Article

Biochemistry **2010,** *49,* 4533–4542 4533
DOI: 10.1021/bi100541t

The Platelet Actin Cytoskeleton Associates with SNAREs and Participates in α-Granule Secretion†

Kamil Woronowicz,‡,∥ James R. Dilks,‡ Nataliya Rozenvayn,‡ Louisa Dowal,‡ Price S. Blair,‡ Christian G. Peters,‡ Lucyna Woronowicz,§ and Robert Flaumenhaft*,‡

‡*Division of Hemostasis and Thrombosis, Department of Medicine, Beth Israel Deaconess Medical Center, Harvard Medical School, Boston, Massachusetts 02215, and* §*Ultrastructure Laboratory, Institute for Basic Research, Staten Island, New York 10314*
∥*Present address: Department of Molecular Biology and Biochemistry, Rutgers University, Piscataway, NJ 08854*

Received April 9, 2010; Revised Manuscript Received April 29, 2010

ABSTRACT: Following platelet activation, platelets undergo a dramatic shape change mediated by the actin cytoskeleton and accompanied by secretion of granule contents. While the actin cytoskeleton is thought to influence platelet granule secretion, the mechanism for this putative regulation is not known. We found that disruption of the actin cytoskeleton by latrunculin A inhibited α-granule secretion induced by several different platelet agonists without significantly affecting activation-induced platelet aggregation. In a cell-free secretory system, platelet cytosol was required for α-granule secretion. Inhibition of actin polymerization prevented α-granule secretion in this system, and purified platelet actin could substitute for platelet cytosol to support α-granule secretion. To determine whether SNAREs physically associate with the actin cytoskeleton, we isolated the Triton X-100 insoluble actin cytoskeleton from platelets. VAMP-8 and syntaxin-2 associated only with actin cytoskeletons of activated platelets. Syntaxin-4 and SNAP-23 associated with cytoskeletons isolated from either resting or activated platelets. When syntaxin-4 and SNAP-23 were tested for actin binding in a purified protein system, only syntaxin-4 associated directly with polymerized platelet actin. These data show that the platelet cytoskeleton interacts with select SNAREs and that actin polymerization facilitates α-granule release.

The role of the actin cytoskeleton in granule exocytosis is enigmatic. It has been demonstrated to act both as a physical barrier that limits granule secretion and as a positive regulator of membrane fusion and cargo release. The ability of the resting actin cytoskeleton to serve as a barrier to granule secretion has been demonstrated in neutrophils, neurons, chromaffin cells, melanotrophs, pancreatic β cells, and acinar cells (*1*−*6*). We have previously demonstrated that platelet granules are coated with actin and that the actin cytoskeleton impedes platelet dense granule and α-granule release (*7*). Partial disruption of this barrier results in augmented and more rapid release of granule contents from platelets. This actin cytoskeletal barrier may help to prevent unregulated release of thrombogenic substances into the circulation (*7*).

Yet accumulating evidence indicates that actin polymerization can promote membrane fusion. Actin polymerization contributes to homotypic fusion of yeast vacuoles (*8*) and fusion of phagosomes with endocytotic organelles (*9*) as well as secretion of granules from neuroendocrine cells (*6*, *10*, *11*) and mast cells (*12*). In some cells, actomyosin contraction and/or dynamic actin polymerization facilitates transport of secretory granules to the plasma membrane (*13*−*15*). In other systems, actin polymerization is required in a terminal step of membrane fusion, following priming and docking (*8*). Several studies have demonstrated that F-actin interacts directly with components of the secretory machinery (*16*−*21*). Yet the significance of these interactions remains uncertain.

One component of the secretory machinery with which F-actin has been demonstrated to interact is *s*oluble *N*EM-sensitive *a*ttachment protein *re*ceptors (SNAREs).[1] SNAREs are membrane-associated proteins that associate via hydrophobic coiled-coil domains and serve a central function in membrane fusion (*22*). SNAREs can be classified as vesicle-associated SNAREs (vSNAREs), which localize to the outer membrane of vesicles, and target-associated SNAREs (tSNAREs), which localize to the cytosolic leaflet of target membranes. Both vesicle-associated membrane proteins (VAMPs) 3 and 8 are SNAREs that have been demonstrated to function in platelet granule secretion (*23*−*25*); however, VAMP-8 has been demonstrated to be the dominant vSNARE in platelets (*25*, *26*). Platelet tSNAREs with established function in platelet granule secretion include SNAP-23, syntaxin 2, and syntaxin 4 (*23*, *25*, *27*−*30*).

The dramatic morphologic change and granule centralization that occurs upon exposure to a strong agonist have led to speculation that the cytoskeleton provides a contractile force that facilitates granule release (*31*−*33*). Yet this hypothesis

†Supported by NIH Grants HL63250 and HL87203 (R.F.) and T32 HL07917 (K.W., L.D., P.S.B., C.G.P.). R.F. is a recipient of an Established Investigator Award from the American Heart Association and a Special Project Award from Bayer Healthcare.

*Address correspondence to this author. Tel: 617-735-4005. Fax: 617-735-4000. E-mail: rflaumen@bidmc.harvard.edu.

[1]Abbreviations: PMA, phorbol 12-myristate 13-acetate; SNARE, SNAP (soluble *N*-ethylmaleimide-sensitive factor attachment protein) receptor; tSNARE, target membrane SNARE; VAMP, vesicle-associated membrane protein; vSNARE, vesicular SNARE.

Published on Web 04/29/2010

remains unproven. An additional or alternative possibility is that platelet F-actin interacts directly with the secretory machinery in order to elicit granule release. To evaluate this possibility, we have assessed the ability of actin polymerization to support α-granule release in a cell-free secretory system. We have also determined whether platelet SNAREs associate with the actin cytoskeleton and have evaluated which platelet SNAREs directly bind actin. These studies demonstrate that actin polymerization facilitates platelet α-granule secretion, that VAMP-8 and syntaxin-2 associate with the actin cytoskeleton only following platelet activation while syntaxin-4 and SNAP-23 associate with the actin cytoskeleton in resting and activated platelets, and that purified platelet actin binds directly to syntaxin 4.

MATERIALS AND METHODS

Platelet Preparation. Blood was obtained from healthy donors who had not ingested aspirin or NSAIDs in the 2 weeks prior to donation. Platelets were isolated by centrifugation followed by gel filtration of platelet-rich plasma as previously described (*34*).

Recombinant SNARE Proteins. Purified human platelet actin (>99% pure) conjugated to fluorescein was purchased from Cytoskeleton Inc. (Denver, CO). GST-tagged SNARE proteins were obtained by PCR from cDNAs containing human isoforms of syntaxin-4 (residues 1−272), SNAP-23, and VAMP-3 (residues 1−83) (generous gifts from Dr. Amira Klip, University of Toronto) and cloned into pGEX-2T from GE Life Sciences. All solutions were prepared using water purified by reverse-phase osmosis on a Millipore Milli-Q purification water system (Bedford, MA).

Antibodies. Rabbit anti-SNAP-23 antibody directed against the C-terminus of SNAP-23 (DRIDIANARAKKLIDS) and anti-VAMP-3 antibody directed against a peptide consisting of the 12 N-terminal amino acids of VAMP-3 were developed in our laboratory (*24*, *34*). A rabbit antibody directed against VAMP-8 antibody was purchased from Abcam (Cambridge, MA). Goat anti-syntaxin-2 antibody directed against a 19 amino acid portion toward the C-terminus of the cytoplasmic domain of syntaxin-1A was obtained from Santa Cruz Biotechnology (Santa Cruz, CA). Mouse anti-syntaxin-4 antibody was obtained from BD Biosciences (San Jose, CA). Rabbit anti-human β-thromboglobulin antiserum was obtained from Nordic Immunology (Tilburg, The Netherlands). Phycoerythrin- (PE-) conjugated mouse monoclonal anti-P-selectin antibody AC1.2 was purchased from BD Biosciences (San Jose, CA).

Differential Interference Contrast (DIC) Microscopy. Platelets (0.5×10^8 to 1×10^8/mL) were treated with latrunculin A or buffer for 5 min. Platelets were subsequently plated on glass slides and visualized using an Olympus AX70 Provis microscope (Olympus, Melville, NY) with a 60 × 1.4 numerical aperture water-immersion lens. Digital images were captured using a Roper CoolSNAP HQ CCD camera (Roper Scientific, Ottobrun, Germany) and analyzed using Slidebook software (Intelligent Imaging Innovations, Denver, CO) in a 1392 × 1040 pixel format.

Evaluation of FITC-Phalloidin Binding. FITC-phalloidin binding to platelets was used to quantify F-actin content as previously described (*35*, *36*). Gel-filtered platelets were incubated with DMSO or the indicated concentration of latrunculin A for 20 min and subsequently exposed to either buffer or 50 μM SFLLRN at room temperature. Following a 20 min incubation, platelets were fixed with formaldehyde for 30 min at 37 °C, permeabilized with 0.5% Triton X-100, and stained with 10 μM FITC-phalloidin for 1 h at 25 °C. Samples were subsequently analyzed for fluorescence using flow cytometry. Data are expressed as percentage of control of resting platelets that were incubated with vehicle alone. Data represent the mean ± SEM of three experiments performed in triplicate.

Flow Cytometry. Flow cytometry was performed on gel-filtered platelet samples using a Becton Dickinson FACSCalibur flow cytometer (San Jose, CA). Fluorescent channels were set at logarithmic gain, and 1×10^4 particles were acquired for each sample. A 585/42 band-pass filter was used for FL-2 fluorescence to measure PE. For evaluation of FITC-phalloidin staining a 530/30 band-pass filter was used to measure FL1 fluorescence. Data were analyzed using CellQuest software (BD Biosciences) on a MacIntosh PowerPC (Apple, Cupertino, CA).

Platelet Aggregation. Washed platelets were incubated with the indicated concentrations of latrunculin A at room temperature for 20 min and then exposed to SFLLRN or ADP. Aggregation was measured using a Chrono-Log 680 aggregation system (Havertown, PA) as previously described (*37*).

Preparation of α-Granule-Enriched Fraction. Preparation of the α-granule-enriched membrane fraction has been described previously (*24*). Briefly, platelets were obtained from healthy donors. Platelet counts were obtained using a HEMA-VET multispecies hematology analyzer (Drew Scientific, Oxford, CT). For fractionation studies, 2×10^9 platelets in 10 mL were washed three times and disrupted by nitrogen cavitation. Uncavitated platelets were removed by centrifugation at 1000*g* for 10 min, and the supernatant was demonstrated to be devoid of platelets by flow cytometry. The supernatant was then subjected to a second round of cavitation. The cavitate was then separated on an Optiprep (Sigma) step gradient by centrifugation at 40000*g* for 2 h. An α-granule-enriched fraction was collected from a 25%/30% interface and dialyzed into buffer (25 mM PIPES, 2 mM EGTA, 137 mM KCl, 4 mM NaCl, pH 6.8) to a final volume of 5 mL. Marker studies indicated that this fraction was enriched in α-granules (*38*). This fraction also contained surface-connected membranes, which were identified by biotin labeling of platelet surface proteins as previously described (*38*). Platelet cytosol was prepared by subjecting nitrogen cavitate to centrifugation at 100000*g* for 1 h and collecting the supernatant.

Electron Microscopy. To prepare the α-granule-enriched fraction for electron microscopy, material above the 25%/30% Optiprep interface was removed. Material at the 25%/30% interface was then fixed using 2 mL of 2.5% glutaraldehyde in 0.1 M cacodylate overnight. The fixed samples were dehydrated and embedded in epon for ultrathin sectioning as previously described (*39*). Ultrathin sections were doubly stained with uranyl acetate and lead citrate (Reynolds reagent) and visualized on a Hitachi 7500 transmission electron microscope (TEM).

Immunofluorescence Microscopy. Samples were fixed in 4% formaldehyde in PBS and centrifuged onto poly(L-lysine) (1 μg/mL) coated coverslips (500 g, 2.5 min). Fractions were washed briefly in PBS and blocked at room temperature in blocking buffer (10% fetal bovine serum, 1% bovine serum albumin, and 0.05% sodium azide) and then washed in triplicate with PBS. Samples were incubated at 1:100 anti-human CD62P antibody diluted in blocking buffer for 1 h at room temperature. Following triplicate washes, samples were incubated in secondary antibody conjugated to Alexa Fluor 488 at a dilution of 1:250 (room temperature, 1.5 h) followed by the addition of Alexa Fluor 568-phalloidin for 20 min. Following three washes in PBS, coverslips

were mounted onto microscope slides using Aqua-Mount (Polysciences). Samples were visualized using an Olympus BX62 microscope with a 60 × 1.42 numerical aperture oil-immersion lens and captured with an Orca-ER- cooled CCD camera (Hamamatsu). Image acquisitions were controlled by iVision-Mac (Biovision Technologies), and analysis was performed using ImageJ.

Cell-Free Secretory System. To evaluate granule secretion in the α-granule-enriched membrane preparation, a 19 μL α-granule-enriched membrane preparation was incubated in the presence of 2 μL of ATP (final concentration 5 mM) (*7*, *28*, *40*−*42*) and 19 μL of platelet cytosol (final concentration 4 mg/mL) (*9*). Samples of the α-granule-enriched membrane preparation incubated in the presence of buffer alone served as controls. Following a 10 min incubation, 10 μL of reaction mixture was transferred into 5 μL of PE-conjugated anti-P-selectin antibody. Stained samples were evaluated by flow cytometry as described above. β-Thromboglobulin release in the α-granule-enriched membrane preparation was monitored by centrifugation of samples at 40000*g* for 1 h to pellet α-granule-enriched membranes. Supernatants were analyzed for β-thromboglobulin by immunoblot analysis.

Isolation of Platelet Cytoskeleton. Platelet cytoskeleton was isolated as previously described by Fox et al. (*43*). Briefly, washed platelets were lysed at a 1:1 ratio in cold Triton X-100 lysis buffer (2% (v/v) Triton X-100, 10 μM leupeptin, 100 mM benzamidine, 100 mM Tris-HCl, pH 7.4, and Complete Protease Inhibitors Cocktail Tablet; Roche Molecular Biochemicals) and 10 mM EGTA. Cytoplasmic actin filaments were sedimented at 15000*g* for 4 min. SNAREs associated with the cytoskeleton actin filaments were subsequently detected by immunoblot analysis.

Immunoblot Analysis. Samples were diluted in sample buffer at 95 °C for 5 min. Proteins were then separated by sodium dodecyl sulfate−polyacrylamide gel electrophoresis (SDS−PAGE). Immunoblotting was performed using FITC-labeled secondary antibodies and visualized using fluorescence detection on a Typhoon 9400 molecular imager (GE Healthcare, Piscataway, NJ).

Actin Cosedimentation Assay. Purified platelet actin (2 μM) was polymerized in 20 mM Tris, pH 7.0, 0.2 mM DTT, 0.2 mM $CaCl_2$, 100 mM KCl, 2 mM $MgCl_2$, and 2 mM ATP for 30 min at room temperature. Recombinant GST-tagged SNARE proteins (2 μM) were incubated with F-actin for an additional 30 min. To sediment F-actin, samples were centrifuged at 100000*g* for 30 min. Supernatants and pellets were then separated, and pellets were resuspended in SDS loading buffer to reconstitute the volume. Equal volumes of pellet and supernatant were added to each lane of the gels, and proteins were separated by SDS−PAGE.

RESULTS

Effects of Inhibition of Actin Polymerization on Platelet Function. To evaluate the role of actin polymerization on platelet function, we used latrunculin A to disrupt the actin cytoskeleton. Latrunculin A binds monomeric actin, facilitating disassembly of the resting actin cytoskeleton (*44*). The specificity of latrunculin A is evidenced by the observation that a mutation in actin renders yeast resistant to > 500 μM latrunculin A (*45*). Initial studies were performed to assess the effect of latrunculin A on F-actin content in resting and activated platelets using FITC-phalloidin to detect F-actin. As previously described (*38*), activation of platelets resulted in a substantial increase in F-actin formation (Figure 1). F-actin content in both resting and activated platelets was markedly decreased following incubation with 10 μM latrunculin A. Incubation with 200 μM latrunculin A further decreased FITC-phalloidin binding and abrogated activation-dependent F-actin formation.

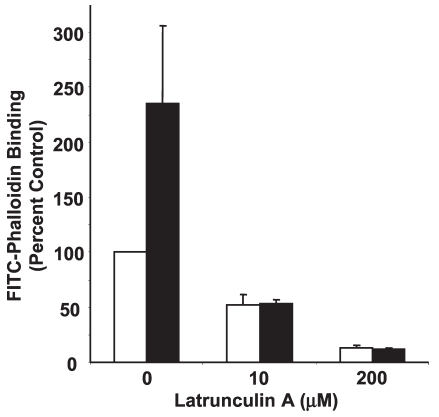

FIGURE 1: Effect of latrunculin A on F-actin content in resting and activated platelets. Gel-filtered platelets were incubated with either vehicle alone, 10 μM latrunculin A, or 200 μM latrunculin A for 20 min and subsequently exposed to either buffer (white bars) or 50 μM SFLLRN (black bars). Following a 10 min incubation, platelets were permeabilized with Triton X-100 and stained with 10 μM FITC-phalloidin. Samples were subsequently analyzed for fluorescence using flow cytometry. Data are expressed as percentage of control of resting platelets that were incubated with vehicle alone.

The effect of disruption of the actin cytoskeleton by latrunculin A on platelet shape change, platelet aggregation, and granule secretion was next evaluated to assess the role of actin in platelet function. To evaluate the effect of cytoskeletal disruption on platelet shape change, platelets were exposed to either buffer alone or 10 or 200 μM latrunculin A and allowed to settle onto glass coverslips. Untreated platelets extended filopodia and had an average area of 39.5 ± 4 μm^2 (Figure 2A, left panel). Platelets exposed to 10 or 200 μM latrunculin A did not extend filopodia and had average areas of 11.3 ± 1.2 μm^2 and 12.4 ± 0.8 μm^2, respectively (Figure 2A, middle and right panels).

The effect of latrunculin A on platelet aggregation was evaluated to assess the role of disassembly of F-actin in platelet activation. Exposure of platelets to 10 μM latrunculin A demonstrated minimal effect on thrombin-induced platelet aggregation (Figure 2B). Exposure to 200 μM latrunculin A resulted in less than 25% inhibition of thrombin-induced platelet activation. Platelet aggregation induced by 5 μM ADP in platelets exposed to 10 or 200 μM latrunculin A was comparable to aggregation in platelets exposed to buffer alone (Figure 2B). These results indicate that even exposure to high concentrations of latrunculin A (i.e., 200 μM) does not result in substantial inhibition of platelet activation as measured by platelet aggregation.

In contrast, F-actin disassembly by latrunculin A had a significant effect on platelet α-granule secretion. P-selectin surface expression was analyzed to monitor α-granule secretion. In the absence of a secretagogue, exposure of platelets to increasing concentrations of latrunculin A resulted in a small increase in P-selectin surface expression (Figure 2C). Thrombin-induced P-selectin expression was slightly augmented following exposure to 10 μM latrunculin A, to 117 ± 13% of the thrombin alone sample. Exposure of platelets to 200 μM latrunculin A, however, inhibited thrombin-induced P-selectin expression to 10 ± 4% of the thrombin alone control. This observation suggests that F-actin contributes to granule secretion.

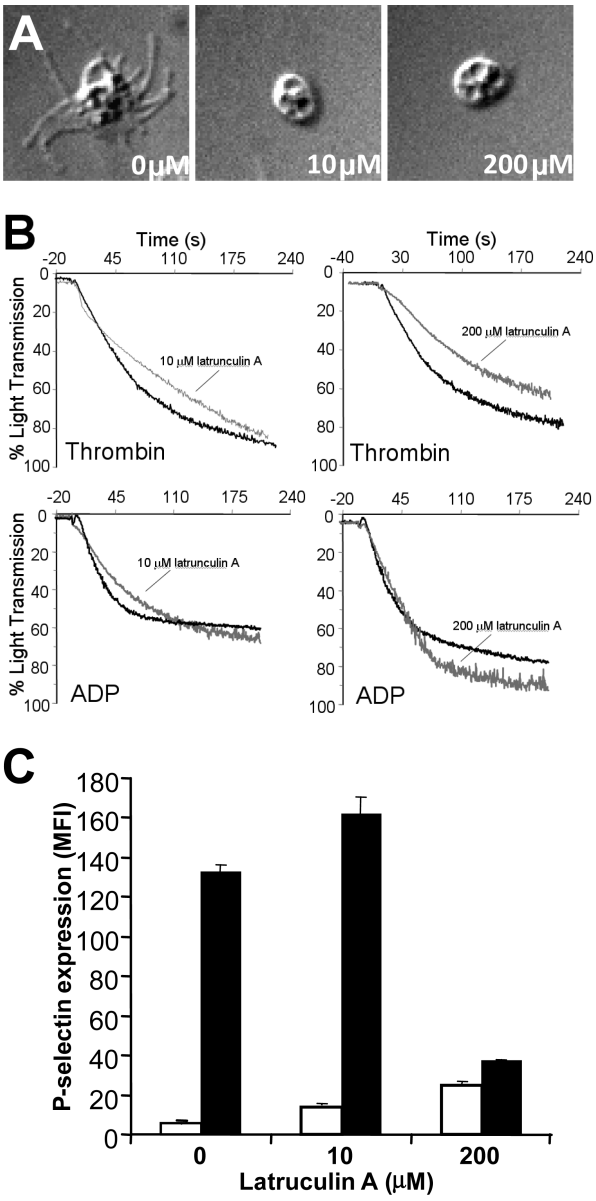

FIGURE 2: Effect of disruption of the actin cytoskeleton on shape change, aggregation, and α-granule secretion. (A) Gel-filtered platelets were incubated with vehicle alone (0 μM), 10 μM latrunculin A (10 μM), or 200 μM latrunculin A (200 μM). Platelets were subsequently plated on glass coverslips and imaged using DIC microscopy. (B) Platelet aggregation was monitored after incubation with either vehicle (black lines) or latrunculin A (gray lines) followed by stimulation with either 1 unit/mL thrombin or 5 μM ADP as indicated. Data are representive tracings from three independent aggregation studies. (C) Gel-filtered platelets were incubated with either vehicle alone, 10 μM latrunculin A, or 200 μM latrunculin A as indicated and subsequently exposed to buffer (white bars) or 1 unit/mL thrombin (black bars). P-selectin surface expression was monitored by flow cytometry. Data represent the mean ± SD of three experiments.

Evaluation of platelet α-granule secretion in response to several different agonists was performed to assess whether latrunculin A inhibited proximal mechanisms involved in α-granule secretion. Exposure of platelets to 10 μM latrunculin A consistently resulted in a slight augmentation of agonist-induced α-granule release (Figure 3). At higher concentrations, however, latrunculin A inhibited α-granule release induced by SFLLRN through protease-activated receptor 1 or by U46619 through the thromboxane prostanoid receptor (Figure 3). Latrunculin A also inhibited

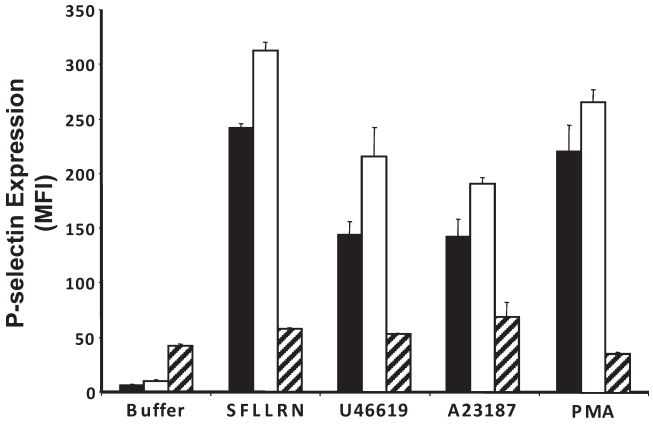

FIGURE 3: Disruption of the actin cytoskeleton inhibits α-granule release induced by distinct agonists. Gel-filtered platelets were incubated with either vehicle alone (black bars), 10 μM latrunculin A (white bars), or 300 μM latrunculin A (hatched bars). Platelets were then exposed to buffer alone, 100 μM SFLLRN, 1 μM U46619, 1 μM A23187, or 0.2 μM PMA and analyzed for P-selectin surface expression by flow cytometry. Data represent the mean ± SD of four to ten experiments.

α-granule secretion induced by the Ca^{2+} ionophore A23187 and by PMA.

Characterization of a Cell-Free Platelet α*-Granule Secretory System*. To evaluate requirements for α-granule secretion, we developed a cell-free platelet α-granule secretory system. An α-granule-enriched fraction was prepared from platelet cavitate as previously described (*38*). Evaluation of the α-granule-enriched cell-free membrane preparation by electron microscopy demonstrated α-granules immediately adjacent to membrane vesicles and membrane fragments (Figure 4A). Occasional isolated α-granules were identified. However, most α-granules were associated with membrane vesicles or fragments. The preparation was devoid of intact platelets or dense granules. α-Granules in this preparation were localized to both the inside of vesicles (Figure 4B,C) and outside of vesicles (Figure 4F,G). α-Granules were also identified adjacent to membrane fragments (Figure 4D,E) and disrupted membrane vesicles (Figure 4F). This arrangement of granules and vesicles is similar to those observed in other granule-enriched fractions used to study granule secretion in cell-free systems (*46*−*48*).

A cell-free platelet α-granule secretory system was modeled after previously described membrane fusion systems (*9*, *46*, *49*−*53*). Platelet cytosol (4 mg/mL) and ATP (5 mM) were incubated with the α-granule-enriched fraction. P-selectin was used as a marker to monitor membrane fusion. P-selectin expression increased several-fold following exposure of the membrane preparation to cytosol and ATP (Figure 5). In contrast, no expression of P-selectin was observed when samples were exposed to either buffer, ATP, or cytosol alone (Figure 5B). No significant increase in the binding of a nonimmune antibody was observed following incubation with cytosol and ATP (data not shown). β-Thromboglobulin, a soluble component of α-granules, was released from the α-granule-enriched preparation upon incubation with ATP and cytosol (Figure 5B, insert). Antibody directed at syntaxin-4, which functions in α-granule secretion (*28*, *54*), inhibited cytosol plus ATP-induced α-granule release by 61 ± 19% (Figure 5C). Antibody directed at the cytoplasmic tail of P-selectin had no significant effect on cytosol plus ATP-induced P-selectin expression. These results indicate that P-selectin exposure in the cell-free system does not result from nonspecific permeabilization of α-granule membranes

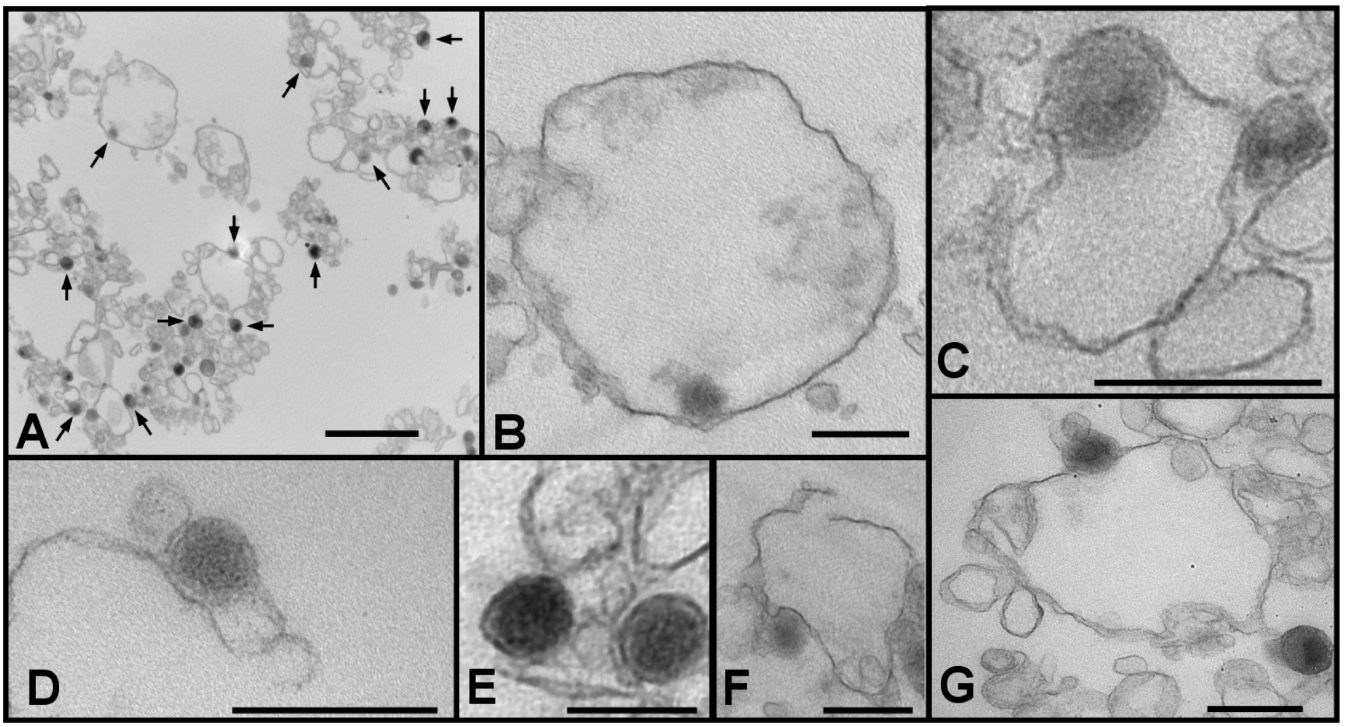

FIGURE 4: Ultrastructure of the α-granule-enriched membrane fraction. (A) Micrograph of the α-granule-enriched preparation demonstrated the presence of abundant α-granules along with other platelet membranes (scale bar, 2 μm). Representative α-granules are indicated by arrows. Nearly all α-granules were associated with membrane structures. α-Granules were found inside membrane vesicles (B, C), associated with membrane fragments (D, E) and disrupted vesicles (F), and identified outside membrane vesicles (G) (scale bars, 0.5 μm).

and that α-granule release in this cell-free system is dependent on cytosol and ATP.

Actin Polymerization in a Cell-Free α-Granule Secretory System. To evaluate the role of actin in platelet α-granule secretion, we determined whether actin polymerization occurred in our α-granule-enriched preparation following incubation with cytosol plus ATP. FITC-phalloidin binding to granules was monitored by flow cytometry. The combination of 4 mg/mL cytosol and 5 mM ATP enhanced the binding of FITC-phalloidin to the α-granule-enriched preparation by approximately 3-fold (Figure 6). In contrast, neither buffer, ATP alone, nor cytosol alone elicited substantial FITC-phalloidin binding when incubated with the α-granule-enriched preparation. FITC-phalloidin binding observed in the presence of ATP plus cytosol was inhibited by incubation of the preparation with cytochalasin B (Figure 6B).

Actin is highly concentrated in platelet cytosol (*55*) and is the most abundant protein in our cytosol preparation. Cytosol may provide a source of actin that enables actin polymerization in the cell-free system. To test this possibility, we determined whether purified actin could replace cytosol in mediating F-actin formation in the α-granule-enriched membrane preparation. For these experiments, the membrane preparation was incubated in the presence of 2 μM purified platelet G-actin covalently coupled to fluorescein. Actin polymerization in platelet granules was monitored by flow cytometry. Incubation of the granule preparation with fluorescein-labeled platelet actin plus 5 mM ATP resulted in actin polymerization (Figure 6C). Actin polymerization was inhibited with cytochalasin E. In contrast, little polymerization was observed when latex beads were incubated in the presence of 2 μM G-actin plus 5 mM ATP in the absence of granules (Figure 6C). Thus, α-granule-enriched membranes facilitate actin polymerization.

Immunofluorescence microscopy was performed to assess the relationship between actin polymerization and P-selectin expression. Two-color immunofluorescence of the untreated α-granule-enriched preparation demonstrated faint staining of both F-actin as detected by Alexa Fluor 568-phalloidin and P-selectin as detected with anti-P-selectin antibody (Figure 7A). Following exposure to ATP plus cytosol, staining of both F-actin and P-selectin increased (Figure 7A). P-selectin expression in samples incubated with ATP plus cytosol was primarily limited to areas of F-actin formation. Quantitative analyses of the images confirmed that both F-actin formation and P-selectin expression increased markedly following exposure to ATP plus cytosol (Figure 7B). Analysis of colocalization of P-selectin and F-actin demonstrated markedly increased colocalization in samples exposed to ATP plus cytosol compared to untreated samples (Figure 7C). Manders' coefficient of colocalization for F-actin and P-selectin in untreated samples was 0.28 ± 0.07, indicating relative segregation of these markers. In the presence of ATP and cytosol, substantial colocalization of these markers was observed as indicated by a Manders' coefficient of 0.90 ± 0.08. These data demonstrate that F-actin in the α-granule-enriched membrane preparation is increased following incubation with ATP and cytosol and that P-selectin expression following exposure to ATP plus cytosol is localized to areas of F-actin formation.

Purified G-Actin Can Substitute for Cytosol To Facilitate α-Granule Secretion in a Cell-Free System. We next determined whether actin polymerization facilitates α-granule secretion in the cell-free secretory system. P-selectin expression observed in the presence of cytosol plus ATP was inhibited by cytochalasin B, indicating a role for actin polymerization in α-granule release (Figure 8A). We then determined whether actin could replace cytosol in enabling α-granule secretion to occur in the cell-free system. Purified platelet G-actin (2 μM) in the

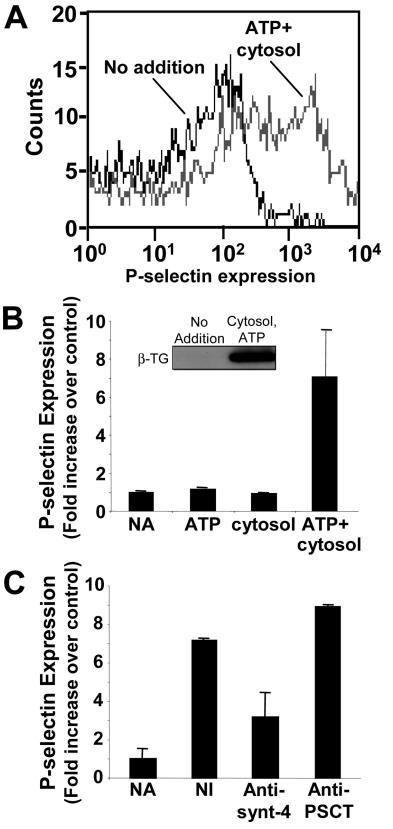

FIGURE 5: P-selectin expression in an α-granule-enriched platelet membrane preparation is dependent on ATP and cytosol. (A) Increased expression of P-selectin is observed following exposure of the α-granule-enriched membrane fraction to 5 mM ATP plus 4 mg/mL platelet cytosol. (B) P-selectin expression was monitored following incubation of the α-granule-enriched membrane fraction with buffer alone (NA), with 5 mM ATP (ATP), with 4 mg/mL platelet cytosol (cytosol), or with ATP plus cytosol (ATP + cytosol). Data represent the mean ± SD of three to four experiments. Insert demonstrates release of β-thromboglobulin from α-granule-enriched fraction following exposure to 4 mg/mL platelet cytosol and 5 mM ATP. (C) P-selectin expression was monitored following incubation of the α-granule-enriched membrane fraction with buffer alone (NA) or in the presence of 5 mM ATP plus 4 mg/mL cytosol following addition of 25 μg/mL of either nonimmune IgG (NI), anti-syntaxin 4 antibody (anti-synt-4), or anti-P-selectin cytoplasmic tail antibody (anti-PSCT). Following a 20 min incubation, the sample was exposed to 5 mM ATP and 4 mg/mL platelet cytosol and analyzed for P-selectin expression by flow cytometry. Data represent the mean ± SD of three experiments.

presence of ATP was able to support the expression of P-selectin in the absence of cytosol (Figure 8B). Actin-induced P-selectin expression was inhibited by cytochalasin E. In contrast, actin failed to affect binding of nonimmune antibody to the granule-enriched population. These data demonstrate that platelet actin facilitates P-selectin expression in this cell-free system.

Association of SNAREs with the Platelet Cytoskeleton. The primary SNAREs that mediate platelet α-granule release are VAMP-8, syntaxin-4, syntaxin-2, and SNAP-23 (*23*, *25*, *28*, *29*, *54*, *56*). We next evaluated whether these SNAREs associated with the filamentous actin cytosolic network. Platelet cytoskeletons were prepared by lysis in 1% Triton X-100 in the presence of protease inhibitors and EGTA to preserve the cytoskeleton, followed by centrifugation at 15000*g* (*57*, *58*). VAMP-8, syntaxin-4, syntaxin-2, and SNAP-23 were all identified in supernatant (Figure 9A). SNAP-23 and syntaxin-4, but not syntaxin-2 or VAMP-8, were identified in the pellet (Figure 9A). The association of SNAREs with the filamentous actin cytosolic network was then evaluated before and after activation of platelets. VAMP-8, syntaxin-4, syntaxin-2, and SNAP-23 were identified within the Triton X-100-insoluble fraction sedimented at 15000*g* following activation of platelets through protease-activated receptor-1 (Figure 9B). To determine whether association of SNAREs with the cytoskeleton was dependent on platelet aggregation, experiments were repeated in the presence of 500 μM RGDS. RGDS had no effect on the association of SNAREs with cytoplasmic actin filaments (data not shown). These studies suggest that SNARE isoforms associate differentially with the Triton X-100-insoluble fraction.

SNARE Association with Purified F-Actin. Association of SNAP-23 and syntaxin-4 with the Triton X-100-insoluble resting platelet cytoskeleton could result from direct binding of platelet actin to SNAREs. Alternatively, these SNAREs may associate with the actin cytoskeleton indirectly through proteins that bind actin. To distinguish between these two possibilities, we assessed the ability of recombinant SNAP-23 and syntaxin-4 to bind purified platelet actin. Purified platelet actin was polymerized in the presence of ATP. Platelet F-actin was then incubated with recombinant proteins. Samples were subsequently sedimented by ultracentrifugation and supernatants and pellets analyzed for proteins using Coomassie staining. GST alone did not cosediment with polymerized platelet actin as evidenced by the observation that >90% of GST remained in the supernatant following ultracentrifugation (Figure 10). In contrast, GST-syntaxin-4 cosedimented with purified, polymerized platelet actin. The actin binding protein

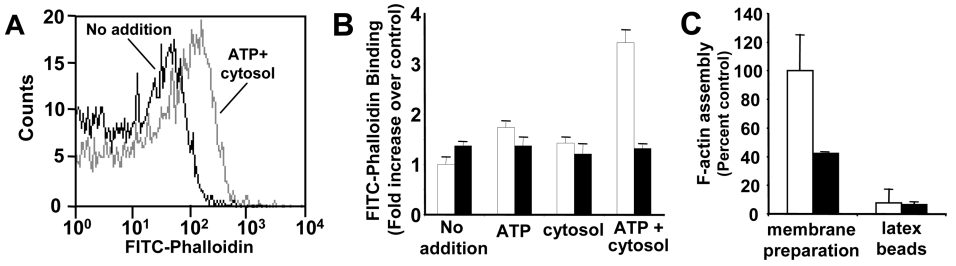

FIGURE 6: Actin polymerization is induced in an α-granule-enriched platelet membrane preparation following incubation with either cytosol or platelet G-actin. (A) The α-granule-enriched membrane fraction was incubated in the presence (gray) or absence (black) of 4 mg/mL platelet cytosol plus 5 mM ATP. Samples were then stained with FITC-phalloidin and evaluated by flow cytometry. (B) The α-granule-enriched membrane preparation was incubated with buffer alone (no addition), 5 mM ATP (ATP), 4 mg/mL cytosol (cytosol), or 5 mM ATP plus 4 mg/mL cytosol (ATP + cytosol) in the presence (black bars) or absence (white bars) of 4 μM cytochalasin B. Samples were subsequently stained with FITC-phalloidin and analyzed by flow cytometry. Data represent the mean ± SD of three to four experiments. (C) The α-granule-enriched membrane fraction or latex beads were incubated in the presence (black bars) or absence (white bars) of 4 μM cytochalasin E. Following a 15 min exposure, samples were exposed to 2 μM fluorescein G-actin plus 5 mM ATP for 30 min. FL-1 fluorescence was subsequently analyzed by flow cytometry. Data represent the mean ± SD of four experiments.

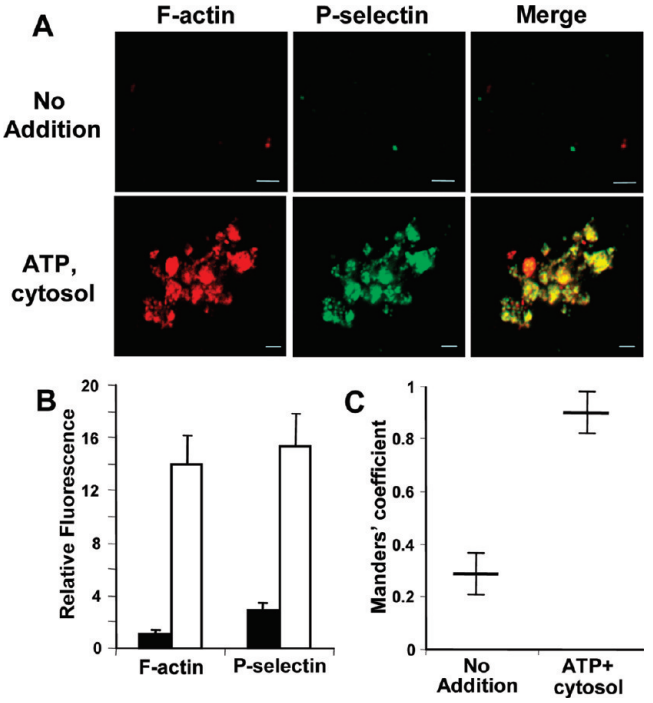

FIGURE 7: Immunofluorescence microscopy of F-actin and P-selectin in an α-granule-enriched preparation. (A) Two-color immunofluorescence was performed to evaluate F-actin using Alexa Flour 568-phalloidin (red), P-selectin using anti-P-selectin antibody (green), and colocalization (yellow). Representative images demonstrate increased staining and colocalization in samples exposed to ATP plus cytosol (ATP, cytosol) compared with untreated samples (no addition). Scale bar is 5 μm. (B) Relative fluorescence of Alexa Fluor 568-phalloidin and anti-P-selectin binding was analyzed in images of samples exposed to ATP plus cytosol (white bars) or untreated samples (black bars). Data represent the mean ± SD of five to seven fields per slide. (C) Colocalization was evaluated using Manders' coefficient in samples exposed to ATP plus cytosol and untreated samples, as indicated. Data represent the mean ± SD of five to seven fields per slide.

α-actinin behaved much like GST-syntaxin-4 in this system, demonstrating significant association with polymerized actin. In comparison, GST-SNAP-23 demonstrated little binding to polymerized platelet actin (Figure 10B). These data indicate that syntaxin-4 binds directly to polymerized platelet actin.

DISCUSSION

These studies indicate that the platelet actin cytoskeleton facilitates granule secretion. Inhibition of actin polymerization with 200 μM latrunculin A did not significantly suppress upstream platelet activation mechanisms as evidenced by the fact that thrombin- or ADP-induced platelet aggregation remained intact. Yet such treatment nearly abolished α-granule release (Figures 1 and 2). Moderate concentrations of latrunculin A (10 μM) augment α-granule release. The observation that an actin inhibitor can have opposite effects on granule secretion depending on its dose is consistent with results in other cell types that demonstrate augmentation of granule release following exposure to moderate doses of actin polymerization inhibitors or depolymerizing proteins but inhibition of exocytosis following exposure to higher doses (*5*, *6*). These observations suggest that disruption of the resting cytoskeleton barrier facilitates granule secretion but that some degree of actin polymerization is required for secretion.

To evaluate the role of actin in promoting α-granule secretion, we used a cell-free secretory system (*46*, *59*−*61*). Like other

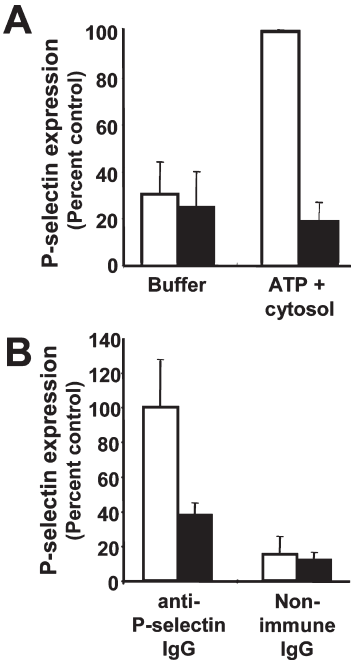

FIGURE 8: Assembly of F-actin mediates P-selectin expression in a cell-free secretory system. (A) The platelet α-granule-enriched membrane preparation was incubated with buffer alone (buffer) or with 5 mM ATP plus 4 mg/mL cytosol (ATP + cytosol) in the presence (black bars) or absence (white bars) of 4 μM cytochalasin B and subsequently analyzed for P-selectin expression by flow cytometry. Data represent the mean ± SD of three experiments. (B) α-Granule-enriched membrane fractions were treated in the presence (black bars) or absence (white bars) of 4 μM cytochalasin E. Samples were subsequently incubated with 2 μM G-actin and 5 mM ATP and assayed for P-selectin expression by flow cytometry. Data represent the mean ± SD of three experiments.

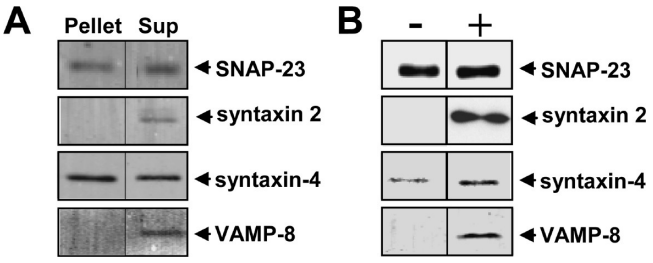

FIGURE 9: Association of SNAREs with the platelet cytoskeleton. (A) Platelets were lysed in 1.5 mL of Triton X-100 lysis buffer at 4 °C. Samples were subjected to centrifugation at 15000*g* to isolate the platelet cytoskeletal actin network. The supernatant was removed and the pellet washed. Samples of the pellet (pellet, 30% of total) and the supernatant (sup, 1% of total) were solubilized in sample buffer and proteins within the samples separated by SDS−PAGE. SNAP-23, syntaxin-2, syntaxin-4, and VAMP-8 within the samples were detected by immunoblot analysis. (B) Platelets were incubated in the presence (+) or absence (−) of SFLLRN and lysed in Triton X-100 lysis buffer containing EGTA. Lysates were then spun at 15000*g*. Proteins in the pellet were separated by SDS−PAGE and analyzed for SNAP-23, syntaxin-2, syntaxin-4, and VAMP-8 by immunoblot analysis.

cell-free secretory systems, the platelet system was dependent on both cytosol and ATP. GTP was not a requirement of this secretory system. In this regard, membrane fusion in this system was more similar to that observed in the latex phagosome system (*62*), which undergoes ATP-dependent membrane fusion in the absence of GTP, than to GTPase-mediated fusion systems. The phagosome membrane fusion system is dependent on *de novo*

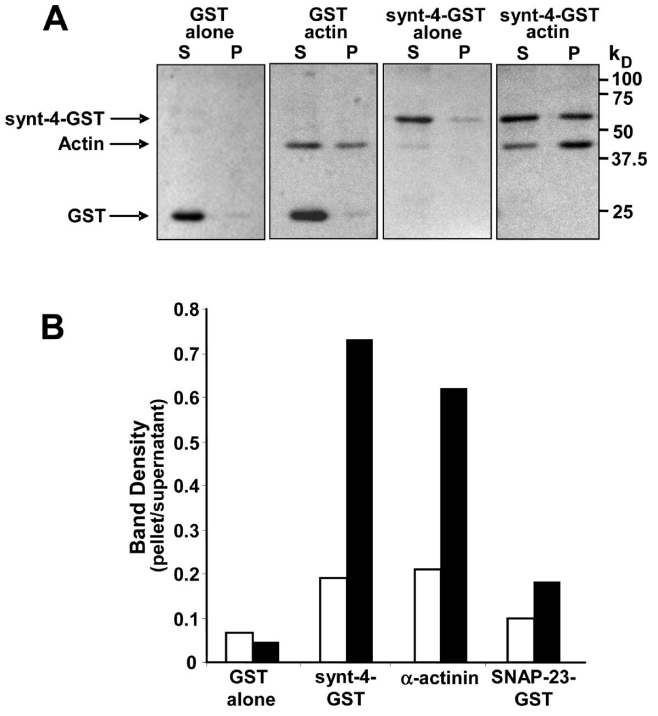

FIGURE 10: A recombinant cytosolic domain of syntaxin-4 binds polymerized platelet actin. (A) Proteins were incubated alone (GST alone; synt-4-GST alone) or in the presence of polymerized platelet actin (GST, actin; synt-4-GST, actin). Samples were pelleted by centrifugation. Proteins within supernatants and pellets were separated by SDS−PAGE and visualized by Coomassie blue staining. (B) Recombinant GST alone, syntaxin-4-GST, α-actinin, or SNAP-23-GST was incubated in the presence (black bars) or absence (white bars) of polymerized platelet actin. Samples were pelleted and proteins within the supernatants and pellets separated by SDS−PAGE. Bands corresponding to each of the proteins were quantified by densitometry. Data represent the ratio of band density in the pellet compared to that in the supernatant and are representative of three to five experiments.

synthesis of PIP_2 for actin assembly (*9*, *62*). Previous studies from our laboratory demonstrate a role for PIP_2 synthesis in platelet α-granule fusion (*41*, *63*). Localized PIP_2 synthesis in platelets may contribute to actin polymerization and thereby facilitate membrane fusion. A role for actin polymerization in cell-free membrane fusion has also been observed in a yeast vacuole system (*8*, *21*). α-Granule release in the platelet cell-free system was blocked by inhibitors of actin polymerization and supported by actin in the absence of cytosol (Figure 8). These data support the premise that actin polymerization facilitates platelet α-granule secretion and raise the question of how F-actin facilitates membrane fusion.

Actin polymerization can contribute to granule secretion by transport of granules to surface-connected membranes (*13*−*15*, *64*) and/or by participating in a terminal step of membrane fusion (*6*, *8*−*12*). Actin has been demonstrated to associate with granules from many cell types, including platelets, pancreatic acinar cells, chromaffin cells, phagosomes, yeast, and others (*7*, *13*, *65*). In many instances, granule membranes serve as sites of assembly of F-actin (*9*, *13*, *66*−*68*). In platelets, actin surrounds isolated α-granules (*7*), and the α-granule-enriched membrane preparation stimulates actin polymerization in the presence of ATP (Figure 4). In yeast and neuroendocrine cells, proteins with established importance in agonist-induced actin polymerization such as Rho proteins and Cdc42 associate with isolated granules and participate in membrane fusion (*8*, *10*, *17*, *21*, *69*). Actin associated with granules could distort or destabilize lipid bilayers as a prerequisite for fusion (*8*). Assembly of F-actin that occurs around fusing granules may serve to stabilize and compress granules (*70*−*72*). Alternatively, actin may control fusion pore dynamics (*73*). Actin binds proteins involved in membrane fusion (*18*, *19*, *21*), and actin remodeling may provide spatial constraints that restrict the secretory machinery to sites of membrane fusion (*74*).

The observation that SNAREs interact with the platelet cytoskeleton suggests a means by which the actin cytoskeleton could impart spatial constraints on the secretory machinery. SNAREs have previously been demonstrated to bind either directly or indirectly to actin. SNAP-23, syntaxin-4, and VAMP-2 colocalize to actin-rich membrane ruffles following insulin stimulation of muscle cells (*16*). VAMP-7 colocalizes with actin at sites of outgrowth in neuronal growth cones (*17*). In purified yeast vacuoles, actin depolymerization promotes SNARE interactions, and subsequent actin polymerization is required following *trans* SNARE complex formation (*8*, *75*). This observation suggests that actin is required in a terminal event leading to membrane fusion (*8*, *75*). Certain SNAREs bind directly to F-actin. Syntaxin 4 binds directly to both F-actin (*18*, *20*) and the membrane skeletal protein, fodrin (*76*, *77*). The yeast R-SNAREs Ykt6p1 and Nyvp1, which both contain longin domains, bind F-actin (*21*).

We demonstrate an association of platelet SNAREs with the F-actin cytosolic network. A limitation of our methodology is that we cannot determine with certainty the concentration of SNAREs associated with the platelet cytoskeleton, since we do not know that it has been isolated in its entirety. These results indicate, however, that SNAP-23, VAMP-8, syntaxin 2, and syntaxin 4 associate with the platelet cytoskeleton (Figure 9). Of these SNAREs, however, only syntaxin 4 binds directly to platelet actin (Figure 10). Syntaxin-4 associates with the cytoskeleton both before and after activation since it binds directly to F-actin. SNAP-23 interacts with syntaxin-4 in resting platelets (*34*, *78*) and may associate with the resting filamentous actin cytosolic network indirectly via this interaction. VAMP-8 and syntaxin-2 only associate with the filamentous actin cytosolic network following platelet activation. The association of VAMP-8 and syntaxin-2 may be indirect and result in part from activation induced by binding to syntaxin-4 and SNAP-23, respectively.

We have previously demonstrated that the platelet cytoskeleton can function as a barrier to granule release (*7*). How might actin act both as a negative and as a positive regulator of platelet granule release? One possibility is that, in the resting state, granules are in close apposition to surface-connected membranes, but fusion is prevented by an intact membrane skeleton, consisting largely of α-adducin, spectrin, and short actin filaments (*79*, *80*) as well as by the resting cytosolic actin cytoskeleton. Upon platelet activation, remodeling of the cytoskeleton including destabilization of the membrane skeleton and *de novo* actin polymerization could ensue. Newly formed actin filaments originating from the granules may tether granule and surface-connected membranes. The association of SNAREs with actin tethers could facilitate SNARE complex formation and subsequent membrane fusion.

REFERENCES

1. Morales, M., Colicos, M. A., and Goda, Y. (2000) Actin-dependent regulation of neurotransmitter release at central synapses. *Neuron 27*, 539–550.
2. Vitale, M. L., Rodriguez Del Castillo, A., Tchakarov, L., and Trifaro, J. M. (1991) Cortical filamentous actin disassembly and scinderin redistribution during chromaffin cell stimulation precede exocytosis, a phenomenon not exhibited by gelsolin. *J. Cell Biol. 113*, 1057–1067.

3. Chowdhury, H. H., Kreft, M., and Zorec, R. (2002) Distinct effect of actin cytoskeleton disassembly on exo- and endocytic events in a membrane patch of rat melanotrophs. *J. Physiol. 545*, 879–886.
4. Jog, N. R., Rane, M. J., Lominadze, G., Luerman, G. C., Ward, R. A., and McLeish, K. R. (2007) The actin cytoskeleton regulates exocytosis of all neutrophil granule subsets. *Am. J. Physiol. Cell Physiol. 292*, C1690–C1700.
5. Orci, L., Gabbay, K. H., and Malaisse, W. J. (1972) Pancreatic beta-cell web: its possible role in insulin secretion. *Science 175*, 1128–1130.
6. Muallem, S., Kwiatkowska, K., Xu, X., and Yin, H. L. (1995) Actin filament disassembly is a sufficient final trigger for exocytosis in nonexcitable cells. *J. Cell Biol. 128*, 589–598.
7. Flaumenhaft, R., Dilks, J. R., Rozenvayn, N., Monahan-Earley, R. A., Feng, D., and Dvorak, A. M. (2005) The actin cytoskeleton differentially regulates platelet alpha-granule and dense-granule secretion. *Blood 105*, 3879–3887.
8. Eitzen, G., Wang, L., Thorngren, N., and Wickner, W. (2002) Remodeling of organelle-bound actin is required for yeast vacuole fusion. *J. Cell Biol. 158*, 669–679.
9. Jahraus, A., Egeberg, M., Hinner, B., Habermann, A., Sackman, E., Pralle, A., Faulstich, H., Rybin, V., Defacque, H., and Griffiths, G. (2001) ATP-dependent membrane assembly of F-actin facilitates membrane fusion. *Mol. Biol. Cell 12*, 155–170.
10. Gasman, S., Chasserot-Golaz, S., Malacombe, M., Way, M., and Bader, M. F. (2004) Regulated exocytosis in neuroendocrine cells: a role for subplasmalemmal Cdc42/N-WASP-induced actin filaments. *Mol. Biol. Cell 15*, 520–531.
11. Malacombe, M., Ceridono, M., Calco, V., Chasserot-Golaz, S., McPherson, P. S., Bader, M. F., and Gasman, S. (2006) Intersectin-1L nucleotide exchange factor regulates secretory granule exocytosis by activating Cdc42. *EMBO J. 25*, 3494–3503.
12. Pendleton, A., and Koffer, A. (2001) Effects of latrunculin reveal requirements for the actin cytoskeleton during secretion from mast cells. *Cell Motil. Cytoskeleton 48*, 37–51.
13. Valentijn, J. A., Valentijn, K., Pastore, L. M., and Jamieson, J. D. (2000) Actin coating of secretory granules during regulated exocytosis correlates with the release of rab3D. *Proc. Natl. Acad. Sci. U.S.A. 97*, 1091–1095.
14. Varadi, A., Tsuboi, T., and Rutter, G. A. (2005) Myosin Va transports dense core secretory vesicles in pancreatic MIN6 beta-cells. *Mol. Biol. Cell 16*, 2670–2680.
15. Rudolf, R., Kogel, T., Kuznetsov, S. A., Salm, T., Schlicker, O., Hellwig, A., Hammer, J. A., 3rd, and Gerdes, H. H. (2003) Myosin Va facilitates the distribution of secretory granules in the F-actin rich cortex of PC12 cells. *J. Cell Sci. 116*, 1339–1348.
16. Tong, P., Khayat, Z. A., Huang, C., Patel, N., Ueyama, A., and Klip, A. (2001) Insulin-induced cortical actin remodeling promotes GLUT4 insertion at muscle cell membrane ruffles. *J. Clin. Invest. 108*, 371–381.
17. Alberts, P., Rudge, R., Irinopoulou, T., Danglot, L., Gauthier-Rouviere, C., and Galli, T. (2006) Cdc42 and actin control polarized expression of TI-VAMP vesicles to neuronal growth cones and their fusion with the plasma membrane. *Mol. Biol. Cell 17*, 1194–1203.
18. Band, A. M., Ali, H., Vartiainen, M. K., Welti, S., Lappalainen, P., Olkkonen, V. M., and Kuismanen, E. (2002) Endogenous plasma membrane t-SNARE syntaxin 4 is present in rab11 positive endosomal membranes and associates with cortical actin cytoskeleton. *FEBS Lett. 531*, 513–519.
19. Thurmond, D. C., Gonelle-Gispert, C., Furukawa, M., Halban, P. A., and Pessin, J. E. (2003) Glucose-stimulated insulin secretion is coupled to the interaction of actin with the t-SNARE (target membrane soluble N-ethylmaleimide-sensitive factor attachment protein receptor protein) complex. *Mol. Endocrinol. 17*, 732–742.
20. Jewell, J. L., Luo, W., Oh, E., Wang, Z., and Thurmond, D. C. (2008) Filamentous actin regulates insulin exocytosis through direct interaction with syntaxin 4. *J. Biol. Chem. 283*, 10716–10726.
21. Isgandarova, S., Jones, L., Forsberg, D., Loncar, A., Dawson, J., Tedrick, K., and Eitzen, G. (2007) Stimulation of actin polymerization by vacuoles via Cdc42p-dependent signaling. *J. Biol. Chem. 282*, 30466–30475.
22. Jahn, R., and Scheller, R. H. (2006) SNAREs—Engines for membrane fusion. *Nat. Rev. Mol. Cell. Biol. 7*, 631–643.
23. Polgar, J., Chung, S. H., and Reed, G. L. (2002) Vesicle-associated membrane protein 3 (VAMP-3) and VAMP-8 are present in human platelets and are required for granule secretion. *Blood 100*, 1081–1083.
24. Feng, D., Crane, K., Rozenvayn, N., Dvorak, A. M., and Flaumenhaft, R. (2002) Subcellular distribution of 3 functional SNARE proteins: Human cellubrevin, SNAP-23, and syntaxin 2. *Blood 99*, 4006–4014.
25. Ren, Q., Barber, H. K., Crawford, G. L., Karim, Z. A., Zhao, C., Choi, W., Wang, C. C., Hong, W., and Whiteheart, S. W. (2007) Endobrevin/VAMP-8 is the primary v-SNARE for the platelet release reaction. *Mol. Biol. Cell 18*, 24–33.
26. Graham, G. J., Ren, Q., Dilks, J. R., Blair, P., Whiteheart, S. W., and Flaumenhaft, R. (2009) Endobrevin/VAMP-8-dependent dense granule release mediates thrombus formation in vivo. *Blood 114*, 1083–1090.
27. Lemons, P. P., Chen, D., Bernstein, A. M., Bennett, M. K., and Whiteheart, S. W. (1997) Regulated secretion in platelets: identification of elements of the platelet exocytosis machinery. *Blood 90*, 1490–1500.
28. Flaumenhaft, R., Croce, K., Chen, E., Furie, B., and Furie, B. C. (1999) Proteins of the exocytotic core complex mediate platelet alpha-granule secretion. Roles of vesicle-associated membrane protein, SNAP-23, and syntaxin 4. *J. Biol. Chem. 274*, 2492–2501.
29. Polgar, J., Lane, W. S., Chung, S. H., Houng, A. K., and Reed, G. L. (2003) Phosphorylation of SNAP-23 in activated human platelets. *J. Biol. Chem. 278*, 44369–44376.
30. Chen, D., Bernstein, A. M., Lemons, P. P., and Whiteheart, S. W. (2000) Molecular mechanisms of platelet exocytosis: role of SNAP-23 and syntaxin 2 in dense core granule release. *Blood 95*, 921–929.
31. Painter, R. G., and Ginsberg, M. H. (1984) Centripetal myosin redistribution in thrombin-stimulated platelets. Relationship to platelet factor 4 secretion. *Exp. Cell Res. 155*, 198–212.
32. Gerrard, J. M., Israels, S. J., and Friesen, L. L. (1985) Protein phosphorylation and platelet secretion. *Nouv. Rev. Fr. Hematol. 27*, 267–273.
33. White, J. G., and Gerrard, J. M. (1978) Recent advances in platelet structural physiology. *Thromb. Haemostasis, Suppl. 63*, 49–60.
34. Flaumenhaft, R., Rozenvayn, N., Feng, D., and Dvorak, A. M. (2007) SNAP-23 and syntaxin-2 localize to the extracellular surface of the platelet plasma membrane. *Blood 110*, 1492–1501.
35. Hartwig, J. H., Kung, S., Kovacsovics, T., Janmey, P. A., Cantley, L. C., Stossel, T. P., and Toker, A. (1996) D3 phosphoinositides and outside-in integrin signaling by glycoprotein IIb-IIIa mediate platelet actin assembly and filopodial extension induced by phorbol 12-myristate 13-acetate. *J. Biol. Chem. 271*, 32986–32993.
36. Kovacsovics, T. J., Bachelot, C., Toker, A., Vlahos, C. J., Duckworth, B., Cantley, L. C., and Hartwig, J. H. (1995) Phosphoinositide 3-kinase inhibition spares actin assembly in activating platelets but reverses platelet aggregation. *J. Biol. Chem. 270*, 11358–11366.
37. Sim, D. S., Dilks, J. R., and Flaumenhaft, R. (2007) Platelets possess and require an active protein palmitoylation pathway for agonist-mediated activation and in vivo thrombus formation. *Arterioscler. Thromb. Vasc. Biol. 27*, 1478–1485.
38. Feng, D., Crane, K., Rozenvayn, N., Dvorak, A. M., and Flaumenhaft, R. (2002) Subcellular distribution of 3 functional platelet SNARE proteins: human cellubrevin, SNAP-23, and syntaxin 2. *Blood 99*, 40064014.
39. Kieseier, B. C., Wisniewski, K. E., and Goebel, H. H. (1997) The monocyte-macrophage system is affected in lysosomal storage diseases: an immunoelectron microscopic study. *Acta Neuropathol. 94*, 359–362.
40. Flaumenhaft, R., Furie, B., and Furie, B. C. (1999) Alpha-granule secretion from alpha-toxin permeabilized, MgATP-exposed platelets is induced independently by H^+ and Ca^{2+}. *J. Cell. Physiol. 179*, 1–10.
41. Rozenvayn, N., and Flaumenhaft, R. (2001) Phosphatidylinositol 4,5-bisphosphate mediates Ca^{2+}-induced platelet alpha-granule secretion. Evidence for type II phosphatidylinositol 5-phosphate 4-kinase function. *J. Biol. Chem. 276*, 22410–22419.
42. Lai, K. C., and Flaumenhaft, R. (2003) SNARE protein degradation upon platelet activation: calpain cleaves SNAP-23. *J. Cell. Physiol. 194*, 206–214.
43. Fox, J. E., Lipfert, L., Clark, E. A., Reynolds, C. C., Austin, C. D., and Brugge, J. S. (1993) On the role of the platelet membrane skeleton in mediating signal transduction. Association of GP IIb-IIIa, pp60c-src, pp62c-yes, and the p21ras GTPase-activating protein with the membrane skeleton. *J. Biol. Chem. 268*, 25973–25984.
44. Spector, I., Braet, F., Shochet, N. R., and Bubb, M. R. (1999) New anti-actin drugs in the study of the organization and function of the actin cytoskeleton. *Microsc. Res. Tech. 47*, 18–37.
45. Ayscough, K. R., Stryker, J., Pokala, N., Sanders, M., Crews, P., and Drubin, D. G. (1997) High rates of actin filament turnover in budding yeast and roles for actin in establishment and maintenance of cell polarity revealed using the actin inhibitor latrunculin-A. *J. Cell Biol. 137*, 399–416.

46. Martin, T. F., and Kowalchyk, J. A. (1997) Docked secretory vesicles undergo Ca^{2+}-activated exocytosis in a cell-free system. *J. Biol. Chem. 272*, 14447–14453.
47. Burgoyne, R. D. (1984) Mechanisms of secretion from adrenal chromaffin cells. *Biochim. Biophys. Acta 779*, 201–216.
48. de Curtis, I., and Simons, K. (1989) Isolation of exocytic carrier vesicles from BHK cells. *Cell 58*, 719–727.
49. Jahraus, A., Tjelle, T. E., Berg, T., Habermann, A., Storrie, B., Ullrich, O., and Griffiths, G. (1998) In vitro fusion of phagosomes with different endocytic organelles from J774 macrophages. *J. Biol. Chem. 273*, 30379–30390.
50. Gu, F., Aniento, F., Parton, R. G., and Gruenberg, J. (1997) Functional dissection of COP-I subunits in the biogenesis of multivesicular endosomes. *J. Cell Biol. 139*, 1183–1195.
51. Lenhard, J. M., Kahn, R. A., and Stahl, P. D. (1992) Evidence for ADP-ribosylation factor (ARF) as a regulator of in vitro endosome-endosome fusion. *J. Biol. Chem. 267*, 13047–13052.
52. Kinuta, M., Yamada, H., Abe, T., Watanabe, M., Li, S. A., Kamitani, A., Yasuda, T., Matsukawa, T., Kumon, H., and Takei, K. (2002) Phosphatidylinositol 4,5-bisphosphate stimulates vesicle formation from liposomes by brain cytosol. *Proc. Natl. Acad. Sci. U.S.A. 99*, 2842–2847.
53. Avery, J., Ellis, D. J., Lang, T., Holroyd, P., Riedel, D., Henderson, R. M., Edwardson, J. M., and Jahn, R. (2000) A cell-free system for regulated exocytosis in PC12 cells. *J. Cell Biol. 148*, 317–324.
54. Lemons, P. P., Chen, D., and Whiteheart, S. W. (2000) Molecular mechanisms of platelet exocytosis: requirements for alpha-granule release. *Biochem. Biophys. Res. Commun. 267*, 875–880.
55. Blikstad, I., Markey, F., Carlsson, L., Persson, T., and Lindberg, U. (1978) Selective assay of monomeric and filamentous actin in cell extracts, using inhibition of deoxyribonuclease I. *Cell 15*, 935–943.
56. Bernstein, A. M., and Whiteheart, S. W. (1999) Identification of a cellubrevin/vesicle associated membrane protein 3 homologue in human platelets. *Blood 93*, 571–579.
57. Fox, J. E., Boyles, J. K., Berndt, M. C., Steffen, P. K., and Anderson, L. K. (1988) Identification of a membrane skeleton in platelets. *J. Cell Biol. 106*, 1525–1538.
58. Fox, J. E., Boyles, J. K., Reynolds, C. C., and Phillips, D. R. (1984) Actin filament content and organization in unstimulated platelets. *J. Cell Biol. 98*, 1985–1991.
59. Avery, J., Jahn, R., and Edwardson, J. M. (1999) Reconstitution of regulated exocytosis in cell-free systems: a critical appraisal. *Annu. Rev. Physiol. 61*, 777–807.
60. Nadin, C. Y., Rogers, J., Tomlinson, S., and Edwardson, J. M. (1989) A specific interaction in vitro between pancreatic zymogen granules and plasma membranes: stimulation by G-protein activators but not by Ca^{2+}. *J. Cell Biol. 109*, 2801–2808.
61. Almeida, M. T., Ramalho-Santos, J., Oliveira, C. R., and Pedroso de Lima, M. C. (1997) Evidence that synaptobrevin is involved in fusion between synaptic vesicles and synaptic plasma membrane vesicles. *Biochem. Biophys. Res. Commun. 236*, 184–188.
62. Defacque, H., Bos, E., Garvalov, B., Barret, C., Roy, C., Mangeat, P., Shin, H. W., Rybin, V., and Griffiths, G. (2002) Phosphoinositides regulate membrane-dependent actin assembly by latex bead phagosomes. *Mol. Biol. Cell 13*, 1190–1202.
63. Rozenvayn, N., and Flaumenhaft, R. (2003) Protein kinase C mediates translocation of type II phosphatidylinositol 5-phosphate 4-kinase required for platelet alpha-granule secretion. *J. Biol. Chem. 278*, 8126–8134.
64. Lang, T., Wacker, I., Wunderlich, I., Rohrbach, A., Giese, G., Soldati, T., and Almers, W. (2000) Role of actin cortex in the subplasmalemmal transport of secretory granules in PC-12 cells. *Biophys. J. 78*, 2863–2877.
65. Fowler, V. M., and Pollard, H. B. (1982) In vitro reconstitution of chromaffin granule-cytoskeleton interactions: ionic factors influencing the association of F-actin with purified chromaffin granule membranes. *J. Cell. Biochem. 18*, 295–311.
66. Wilkins, J. A., and Lin, S. (1981) Association of actin with chromaffin granule membranes and the effect of cytochalasin B on the polarity of actin filament elongation. *Biochim. Biophys. Acta 642*, 55–66.
67. Defacque, H., Egeberg, M., Habermann, A., Diakonova, M., Roy, C., Mangeat, P., Voelter, W., Marriott, G., Pfannstiel, J., Faulstich, H., and Griffiths, G. (2000) Involvement of ezrin/moesin in de novo actin assembly on phagosomal membranes. *EMBO J. 19*, 199–212.
68. Defacque, H., Egeberg, M., Antzberger, A., Ansorge, W., Way, M., and Griffiths, G. (2000) Actin assembly induced by polylysine beads or purified phagosomes: quantitation by a new flow cytometry assay. *Cytometry 41*, 46–54.
69. Bader, M. F., Doussau, F., Chasserot-Golaz, S., Vitale, N., and Gasman, S. (2004) Coupling actin and membrane dynamics during calcium-regulated exocytosis: a role for Rho and ARF GTPases. *Biochim. Biophys. Acta 1742*, 37–49.
70. Sokac, A. M., Co, C., Taunton, J., and Bement, W. (2003) Cdc42-dependent actin polymerization during compensatory endocytosis in *Xenopus* eggs. *Nat. Cell Biol. 5*, 727–732.
71. Yu, H. Y., and Bement, W. M. (2007) Control of local actin assembly by membrane fusion-dependent compartment mixing. *Nat. Cell Biol. 9*, 149–159.
72. Nemoto, T., Kojima, T., Oshima, A., Bito, H., and Kasai, H. (2004) Stabilization of exocytosis by dynamic F-actin coating of zymogen granules in pancreatic acini. *J. Biol. Chem. 279*, 37544–37550.
73. Larina, O., Bhat, P., Pickett, J. A., Launikonis, B. S., Shah, A., Kruger, W. A., Edwardson, J. M., and Thorn, P. (2007) Dynamic regulation of the large exocytotic fusion pore in pancreatic acinar cells. *Mol. Biol. Cell 18*, 3502–3511.
74. Eitzen, G. (2003) Actin remodeling to facilitate membrane fusion. *Biochim. Biophys. Acta 1641*, 175–181.
75. Wang, L., Merz, A. J., Collins, K. M., and Wickner, W. (2003) Hierarchy of protein assembly at the vertex ring domain for yeast vacuole docking and fusion. *J. Cell Biol. 160*, 365–374.
76. Nakano, M., Nogami, S., Sato, S., Terano, A., and Shirataki, H. (2001) Interaction of syntaxin with alpha-fodrin, a major component of the submembranous cytoskeleton. *Biochem. Biophys. Res. Commun. 288*, 468–475.
77. Liu, L., Jedrychowski, M. P., Gygi, S. P., and Pilch, P. F. (2006) Role of insulin-dependent cortical fodrin/spectrin remodeling in glucose transporter 4 translocation in rat adipocytes. *Mol. Biol. Cell 17*, 4249–4256.
78. Chung, S. H., Polgar, J., and Reed, G. L. (2000) Protein kinase C phosphorylation of syntaxin 4 in thrombin-activated human platelets. *J. Biol. Chem. 275*, 25286–25291.
79. Gilligan, D. M., Sarid, R., and Weese, J. (2002) Adducin in platelets: activation-induced phosphorylation by PKC and proteolysis by calpain. *Blood 99*, 2418–2426.
80. Barkalow, K. L., Italiano, J. E., Jr., Chou, D. E., Matsuoka, Y., Bennett, V., and Hartwig, J. H. (2003) {alpha}-Adducin dissociates from F-actin and spectrin during platelet activation. *J. Cell Biol. 161*, 557–570.